Research Article | Vol. 29, No. 11 / 24 May 2021 / Optics Express 17428
Optics EXPRESS

Information rates in Kerr nonlinearity limited optical fiber communication systems

TIANHUA XU,[1,2,3,5] NIKITA A. SHEVCHENKO,[4,6] YUNFAN ZHANG,[1] CENQIN JIN,[2] JIAN ZHAO,[1,7] AND TIEGEN LIU[1]

[1]School of Precision Instruments & Opto-Electronics Engineering, Tianjin University, Tianjin 300072, China
[2]School of Engineering, University of Warwick, Coventry CV4 7AL, UK
[3]Department of Electronic & Electrical Engineering, University College London, London WC1E7JE, UK
[4]Department of Engineering, University of Cambridge, Cambridge CB3 0FA, UK
[5]tianhua.xu@ieee.org
[6]ms2688@cam.ac.uk
[7]enzhaojian@tju.edu.cn

Abstract: Achievable information rates of optical communication systems are inherently limited by nonlinear distortions due to the Kerr effect occurred in optical fibres. These nonlinear impairments become more significant for communication systems with larger transmission bandwidths, closer channel spacing and higher-order modulation formats. In this paper, the efficacy of nonlinearity compensation techniques, including both digital back-propagation and optical phase conjugation, for enhancing achievable information rates in lumped EDFA- and distributed Raman-amplified fully-loaded C −band systems is investigated considering practical transceiver limitations. The performance of multiple modulation formats, such as dual-polarisation quadrature phase shift keying (DP-QPSK), dual-polarisation 16 −ary quadrature amplitude modulation (DP-16QAM), DP-64QAM and DP-256QAM, has been studied in C −band systems with different transmission distances. It is found that the capabilities of both nonlinearity compensation techniques for enhancing achievable information rates strongly depend on signal modulation formats as well as target transmission distances.

1. Introduction

It is widely accepted that over 95% of currently estimated digital data traffic is carried over optical fibre networks forming a substantial part of the national and international communication infrastructure [1,2]. A soft-decision decoding and advanced modulation formats are the key technologies to increase data rates in optical communication networks. The achievable information rate (AIR) is a natural figure of merit in coded communication systems, which demonstrates the net data rates achieved assuming the ideal error corrections [3–6]. Since linear impairments, such as chromatic dispersion (CD), polarisation mode dispersion (PMD), and laser phase noise can be well compensated via digital signal processing [7–9], AIRs of optical transmission systems are still limited by nonlinear distortions due to the Kerr effect in optical fibres [10,11]. These impairments are appeared to be more significant for communication systems with wider transmission bandwidths, closer channel spacing, as well as higher-order modulation formats [10–13].

Digital nonlinearity compensation (NLC) and optical nonlinearity compensation techniques, such as digital back-propagation (DBP) and optical phase conjugation (OPC), have been developed to mitigate both intra-channel and inter-channel fibre nonlinearities [12–16]. These techniques have been validated to effectively improve the signal-to-noise ratios (SNRs) or Q^2 factors

#415753 https://doi.org/10.1364/OE.415753
Journal © 2021 Received 24 Nov 2020; revised 27 Apr 2021; accepted 10 May 2021; published 21 May 2021

Optics EXPRESS

in single-channel and multi-channel long-haul optical communication systems [13–22]. To reveal the net data rates that can be achieved, research has been carried out to study the performance of multi-channel nonlinearity compensation (MC-NLC) in terms of AIRs in optical communication systems [5,23–25]. In our previous work, fully-loaded EDFA and ideal Raman amplified systems were investigated from the perspective of achievable information rates for the digital back-propagation scheme [12,26,27]. This paper extends the scope of the investigation to practical 1$^{\text{st}}$−order distributed Raman amplification (DRA) schemes, and the achievable information rates are examined in the case of NLC systems using both DBP and OPC techniques. In particular, the performance of NLC to enhance AIRs was investigated in C−band (~4.8 THz) Nyquist-spaced wavelength division multiplexing (WDM) transmission systems, using different modulation formats varying from dual-polarisation quadrature phase shift keying (DP-QPSK) to dual-polarisation 256−ary quadrature amplitude modulation (DP-256QAM). Since numerical simulations of fully-loaded C−band systems with a range of modulation formats are computationally intractable, a theoretical model considering modulation format-dependent distortions and transceiver noise limitations was developed to investigate the performance of such systems. This enabled a realistic study of the efficacy of MC-NLC to enhance AIRs for different modulation formats. The model was used to explore the transmission regimes where MC-NLC can have a significant impact on AIRs in C−band systems, and importantly to highlight the required compensation bandwidth.

2. Theoretical model

Considering the contributions from amplified spontaneous emission (ASE) noise, fibre nonlinear distortions (which are due to optical Kerr effect in fibre), as well as practically relevant system transceiver noise limitations, the performance of a dispersion-unmanaged optical communication system, as shown in Fig. 1, can be estimated by introducing the so-called effective SNR [13,28–30], where the nonlinear interference is treated as an additive Gaussian noise with an effective variance of σ^2_{eff}. Thus, the effective SNR after fibre propagation can be approximated as follows

$$\text{SNR} \triangleq \frac{P}{\sigma^2_{\text{eff}}} \approx \frac{P}{\sigma^2_{\text{TR}} + \sigma^2_{\text{ASE}} + \sigma^2_{\text{S-TR}} + \sigma^2_{\text{S-ASE}} + \sigma^2_{\text{S-S}}}, \tag{1}$$

where P denotes the average optical signal power per channel, σ^2_{TR} is the transceiver noise, σ^2_{ASE} is the total power of ASE noise within the examined channel arising from the optical amplifiers, $\sigma^2_{\text{S-S}}$ is the nonlinear distortions due to the four-wave mixing (FWM) among signal frequency components, $\sigma^2_{\text{S-ASE}}$ represents the distortions due to signal-ASE noise nonlinear interaction, and finally $\sigma^2_{\text{S-TR}}$ denotes the nonlinear the beating between signal and transceiver noise [31].

Apart from the lumped EDFA amplification, optical amplification process can be also realised in a distributed fashion. In this case, the signal is amplified by the frequency-separated Raman pumps (the frequency separation between signal and Raman pump is typically up to 15 THz), and thus, the fibre itself plays the role of an active gain medium. The use of only one Raman pump beam is commonly referred to as the 1$^{\text{st}}$−order distributed Raman amplification. Following the approach given in [32], we have derived a closed-form expression in Eq. (2), which allows us to evaluate the ASE noise in the case of the 1$^{\text{st}}$−order DRA (see signal power profiles in Fig. 2). Hence, for multi-span dual-polarisation WDM transmission systems, the overall ASE noise exhibits itself as an additive white Gaussian noise arising either from EDFAs at the end of each fibre span or from optical counter-pumped 1$^{\text{st}}$−order DRA can be respectively evaluated as follows [32–35]

$$\sigma^2_{\text{ASE}} = \begin{cases} N_{\text{s}}\left(e^{\alpha L_{\text{s}}} - 1\right) \cdot \text{NF} \cdot hf_0 \cdot \Delta f, & \text{(EDFA)} \\ 2N_{\text{s}}\left(\kappa_T + 1\right) \mathcal{N}_{\text{phot}} \cdot hf_0 \cdot \Delta f, & \text{(DRA)} \end{cases} \tag{2}$$

Optics EXPRESS

where N_s is the total number of fibre spans in the link, α is the fibre attenuation coefficient, L_s is the fibre span length, NF stands for the EDFA noise figure, hf_0 is the average photon energy at the optical carrier frequency f_0, and Δf is the channel spacing, κ_T is the temperature dependent phonon occupancy factor, and $\mathcal{N}_{\text{phot}}$ is the number of spontaneously emitted photons accounting for signal power profiles achieved by the 1$^{\text{st}}$−order Raman pumping, and can be expressed via the exact closed-form solution as follows

$$\mathcal{N}_{\text{phot}} = \left(\frac{\alpha_{\text{p}}}{g_R P_{\text{p}}}\right)^{\frac{\alpha}{\alpha_p}} \left[\Gamma\left(1+\frac{\alpha}{\alpha_{\text{p}}}, \frac{g_R P_{\text{p}}}{\alpha_{\text{p}}} e^{-\alpha_{\text{p}} L_{\text{s}}}\right) - \Gamma\left(1+\frac{\alpha}{\alpha_{\text{p}}}, \frac{g_R P_{\text{p}}}{\alpha_{\text{p}}}\right)\right] \exp\left(\frac{g_R P_{\text{p}}}{\alpha_{\text{p}}}\right), \tag{3}$$

where g_R is the normalised modal Raman gain coefficient, P_{p} is the launched power of the backward pump beam, α_{p} is the fibre attenuation coefficient corresponding to the Raman pump frequency, $\Gamma(\cdot, x)$ denotes the upper incomplete Gamma function [36]. Hereinafter, the value of backward Raman pump power P_{p} is supposed to be adjusted to entirely compensate for the fibre loss in each fibre span. Additionally, the ASE noise power spectral density is assumed to be ideally flat across the whole signal spectrum, as the effect of the inter-channel stimulated Raman scattering (SRS) in a multi-channel system is usually negligible in the case of C−band transmission [37].

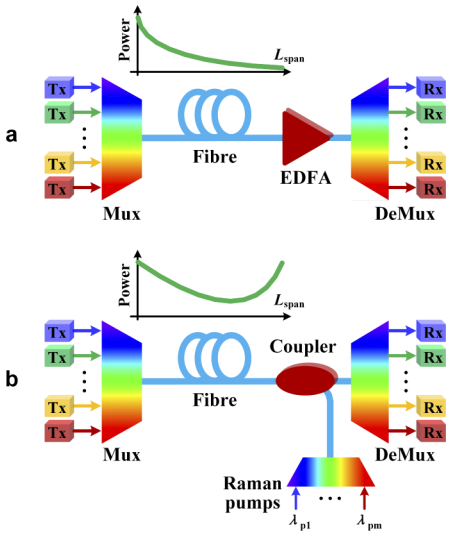

Fig. 1. Schematic of optically amplified WDM communication systems using nonlinearity compensation. **a**. EDFA amplified transmission system and power profile in each fibre span, **b**. Raman (first-order) amplified transmission system and power profile in each fibre span. Tx: transmitter, Rx: receiver, Mux: multiplexer, DeMux: de-multiplexer.

In the absence of nonlinearity mitigation, the contribution of the noisy distortions due to the FWM between signal frequency components is given by the well-known expression [28,29,38–40]

$$\sigma^2_{\text{S-S}} = \eta\,(N_{\text{s}}, B)\cdot P^3, \tag{4}$$

where $\eta\,(N_{\text{s}}, B)$ represents the nonlinear distortion coefficient, which implicitly depends on fibre span length and transmitted bandwidth B. The signal-ASE noise interaction is estimated as shown in Eq. (5). Aside from the 1$^{\text{st}}$−order signal-ASE interaction [41,42], the 2$^{\text{nd}}$-order signal-ASE interaction for both EDFA and DRA schemes is evaluated, similar to procedures in [16,43], as

Optics EXPRESS

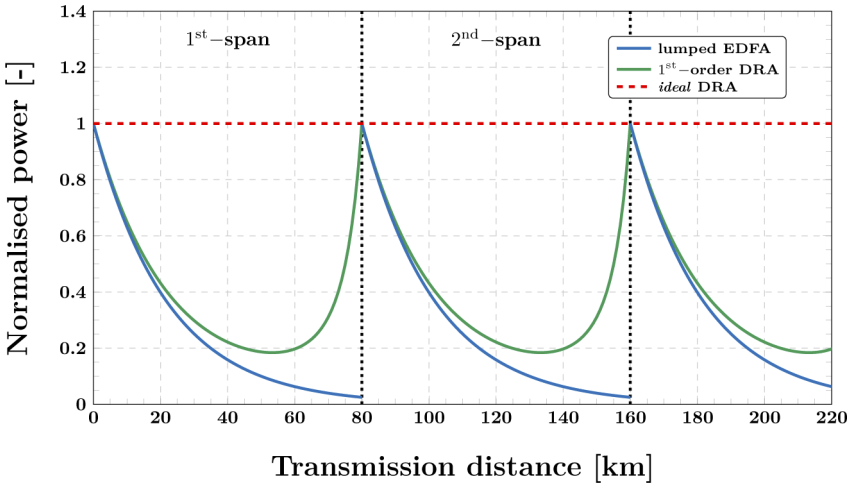

Fig. 2. Signal normalised power profiles considering lumped EDFA (solid blue), counter-propagating 1st−order DRA (solid green), and ideal DRA (dashed red) cases.

follows

$$\sigma^2_{\text{S-ASE}} \approx 3\,\frac{\sigma^2_{\text{ASE}}}{N_{\text{s}}}\sum_{n=1}^{N_{\text{s}}}\left[\eta\,(n,B)+3\sum_{m=1}^{n-1}\eta\,(m,B)\cdot P^2\right]\cdot P^2. \tag{5}$$

It should be emphasised that the partial bandwidth DBP case corresponds to the NLC, which is partially applied over a certain bandwidth (less than transmitted bandwidth), the signal-signal interaction term can then be described as follows [4,12,44]

$$\sigma^2_{\text{S-S}} = \left[\,\eta\,(N_s,B)-\eta\,(N_s,B_{\text{NLC}})\,\right]\cdot P^3, \tag{6}$$

where B_{NLC} represents the NLC bandwidth. It should also be noted that in the optical phase conjugation scheme, one can utilise either full-field OPC or just linear compensation (EDC). Partial-bandwidth compensation cannot be applied in the OPC compensated systems [45,46]. Here we assume a full compensation of the signal-signal interaction in the OPC scheme, and this provides an upper bound of the performance in the considered system.

Following the well-known conventional GN-model approach [28,39,40,47], we considered ideal Nyquist-spaced WDM systems, and the the centre channel nonlinear distortion coefficient η was computed by following double improper integral

$$\begin{aligned}\eta\,(N_s,B) = \frac{16\,\gamma^2}{27\,R_s^2}\int_{-\infty}^{\infty}\int_{-\infty}^{\infty} df_1 df_2\ \text{rect}\left(\frac{f_1+f_2}{B}\right)\\ \cdot\,|\,\varphi\,(f,f_1,f_2\,|\,L_{\text{s}},N_{\text{s}})\cdot\rho\,(f,f_1,f_2\,|\,L_{\text{s}})\,|^{\,2},\end{aligned} \tag{7}$$

where γ is the fibre nonlinearity parameter, R_S denotes the symbol rate of the transmitted signal, $\text{rect}\,(x)$ denotes the rectangular function. The nonlinear interference noise distance evolution is defined by the phased-array factor $\varphi\,(f,f_1,f_2\,|\,L_{\text{s}},N_{\text{s}})$, which takes into account the decorrelation process of nonlinear interactions along the multi-span transmission system [28,47]. The FWM efficiency factor $\rho\,(f,f_1,f_2\,|\,L_{\text{s}})$ has a different expression depending on the used optical amplification scheme. Note that these functions in Eq. (7) are evaluated at the central channel (i.e.,$f=0$), in other words, the power spectral density of nonlinear distortions is assumed to be ideally flat across the whole transmission bandwidth. Here a closed-form expression of the

Optics EXPRESS

FWM efficiency factor is derived corresponding to the signal power profile of the 1st−order DRA shown in Fig. 2. Hence, for lumped EDFA and 1st−order backward-pumped DRA, it respectively yields

$$\rho\left(f,f_1,f_2\,|\,L_{\rm s}\right)=\begin{cases}\frac{1-\exp\left[-\left(\alpha+i\,\Delta\beta(f,f_1,f_2)\right)\cdot L_{\rm s}\right]}{\alpha-i\,\Delta\beta(f,f_1,f_2)}, & \text{(EDFA)}\\ \frac{\Xi(f,f_1,f_2\,|\,L_{\rm s})}{\alpha_{\rm p}}\left(-\frac{g_R P_{\rm p}}{\alpha_{\rm p}}\right)^{\frac{\alpha-i\,\Delta\beta(f,f_1,f_2)}{\alpha_{\rm p}}}\exp\left(-\frac{g_R P_{\rm p}}{\alpha_{\rm p}}\right), & \text{(DRA)}\end{cases} \tag{8}$$

where $i\triangleq\sqrt{-1}$ denotes the imaginary unit. The FWM phase-mismatch factor $\Delta\beta\left(f,f_1,f_2\right)$ includes the effect of both fibre chromatic dispersion (captured by D parameter) and dispersion slope (captured by S parameter), and can be readily found in, e.g., [48]. The following notation was also introduced

$$\begin{aligned}\Xi\left(f,f_1,f_2\,|\,L_{\rm s}\right)\triangleq\Gamma\left(-\frac{\alpha-i\,\Delta\beta\left(f,f_1,f_2\right)}{\alpha_{\rm p}},-\frac{g_R P_{\rm p}}{\alpha_{\rm p}}\,e^{\alpha_{\rm p}L_{\rm s}}\right)\\ -\Gamma\left(-\frac{\alpha-i\,\Delta\beta\left(f,f_1,f_2\right)}{\alpha_{\rm p}},-\frac{g_R P_{\rm p}}{\alpha_{\rm p}}\right).\end{aligned} \tag{9}$$

It should also be emphasised that in order to end up with closed-form expressions of the FWM ρ−factor Eq. (8) in the case of 1st−order DRA, the effect of Raman pump depletion was assumed to be neglected as, in the case of C-band transmission, its contribution is fairly marginal. In addition, no polarisation effects on the Raman gain g_R were considered. The integral in Eq. (7) was evaluated numerically via the multi-variable quasi-Monte-Carlo integration (see, e.g., [49]).

Assuming an equal contribution of transceiver noise arising from both transmitter and receiver, the transceiver noise and the nonlinear interaction between the signal and transceiver noise can be respectively described as follows [31]

$$\sigma^2_{\rm TR}=\mathrm{SNR}^{-1}_{\rm TR}\cdot P, \tag{10}$$

$$\sigma^2_{\text{S-TR}}=\frac{3}{2}\,\mathrm{SNR}^{-1}_{\rm TR}\cdot\sigma^2_{\text{S-S}}, \tag{11}$$

where $\mathrm{SNR}_{\rm TR}$ represents the maximum observable signal-to-noise ratio imposed by the transceiver.

In order to estimate the AIRs, we use soft-decision mutual information (MI) based on an additive white Gaussian noise channel model (AWGN) [5,6] at the optimum launch power regimes (for both EDC and MC-NLC cases) considering dispersion-unmanaged optical communication systems [6,13]. The discrete-time memoryless AWGN channel with complex-valued input random symbols X and output symbols Y in each polarisation is given by simple input-output relationship $X=Y+Z$, where Z denotes the input-independent, complex-valued, identically distributed, zero-mean circularly symmetric Gaussian random variable with the variance, which is assumed to be approximately equal to the effective variance $\sigma^2_{\rm eff}$ within the scope of model Eq. (1). Symbol-wised soft-decision MI can be computed as [3,6]

$$\mathrm{MI}=\frac{1}{|\mathcal{X}|}\sum_{x\in\mathcal{X}}\int_{\mathbb{C}}dy\,p_{Y\,|\,X}\left(y\,|\,x\right)\log_2\frac{p_{Y\,|\,X}\left(y\,|\,x\right)}{\frac{1}{M}\sum_{x'\in\mathcal{X}}p_{Y\,|\,X}\left(y\,|\,x'\right)}, \tag{12}$$

where $|\cdot|$ denotes the cardinality of a set, $\mathcal{X}$ and $\mathbb{C}$ are the set of transmitted random symbols and the set of complex numbers, respectively; $p_{Y\,|\,X}\left(y\,|\,x\right)$ is set to be the zero-mean complex-valued Gaussian conditional probability density function with the $\sigma^2_{\rm eff}$ variance. The MI in was numerically estimated for a centre channel via the Gauss-Hermite quadrature [3,4,6]. Finally, the overall AIR of the considered system is defined as [4–6,12,44].

$$\mathrm{AIR}\triangleq 2N_{\rm ch}R_{\rm S}\cdot\mathrm{MI}\,. \tag{13}$$

Optics EXPRESS

3. Results and discussions

3.1. Digital nonlinearity compensation (digital back-propagation)

Based on the theoretical model above, the AIRs of EDFA-based $C-$band transmission systems have been investigated for the case of electronic dispersion compensation (EDC), partial-bandwidth and full-field digital NLC (FF-NLC). Both the ideal transmission scheme (without a transceiver noise limitation) and a more practical transmission scheme (transceiver SNR of 25 dB) were used to study the performance of NLC in $C-$band optical communication systems. System parameters are detailed in Table 1. Polarisation mode dispersion is assumed to be neglected, since it has been previously shown that the transceiver noise greatly outweighs the impact of PMD [31]. Phase noise from the transmitter and local oscillator lasers, as well as the frequency offset between them are also neglected. In our NLC schemes, 32-GHz refers to the bandwidth of single-channel nonlinear compensation, while 250-GHz refers to current practically possible digital NLC bandwidth [50].

Table 1. Transmission systems parameters.

Parameters	Values
Central wavelength (λ_0)	1550 nm
Symbol rate (R_S)	32 GBd
Channel spacing (Δf)	32 GHz
Number of channels (N_{ch})	151
Attenuation coefficient (α)	0.2 dB/km
CD coefficient (D)	17 ps/nm/km
CD slope coefficient (S)	0.067 ps/nm^2/km
Nonlinear coefficient (γ)	1.2 /W/km
Span length (L_{s})	80 km
EDFA noise figure (NF)	4.5 dB
Raman gain (g_R)	0.35 /W/km
Raman pump loss (α_{p})	0.25 dB/km

Figure 3 illustrates the AIR versus transmission distance for different modulation formats in an ideal $C-$band transmission with DBP. It was found that for DP-QPSK, the systems using EDC, partial-bandwidth and full-field DBP show the same (saturated) AIR, for transmission distances of up to 10,000 km. This suggests that in an ideal $C-$band transmission scheme with DP-QPSK applied, nonlinear compensation is not required to enhance the AIR for system reach up to 10,000 km. For DP-16QAM NLC becomes effective in increasing AIR for transmission distances greater than 2000 km. For DP-64QAM nonlinear compensation increases the AIRs at distances longer than 600 km, while for DP-256QAM DBP is effective for all considered distances starting from 400 km. It is interesting to note that DP-64QAM shows similar AIRs to DP-256QAM with up to 250-GHz NLC, if the distances are longer than 3000 km.

We further examine the impact on AIRs of transceiver noise as a practical consideration. Figure 4 illustrates the AIR versus transmission distance for different modulation formats in $C-$band transmission systems. Here we assume a transceiver SNR of 25 dB to emulate a reasonable state-of-the-art system performance. It is confirmed that nonlinear compensation is not a necessity for enhancing the AIR in DP-QPSK transmission at distances up to 10,000 km. Similar to the case without transceiver noise, for DP-16QAM NLC increases the AIR at transmission distances exceeding 2000 km. However, for DP-64QAM the transceiver noise has an impact on the system reach where the nonlinear compensation becomes effective – it is reduced to less than 400 km. This is also the case for DP-256QAM since applying DBP increases AIRs

Optics EXPRESS

for all examined distances from 400 to 10,000 km. We also observe that for EDC case, 32-GHz and 250-GHz digital NLC, DP-64QAM exhibits very similar AIRs as DP-256QAM system for distances longer than 2000 km. Our investigation shows that in comparison with ideal $C-$band schemes, transceiver noise limitations have a marginal impact on the AIRs of DP-QPSK and DP-16QAM systems, whereas it degrades more significantly the performance of DP-64QAM and DP-256QAM modulation formats.

The case of Raman amplification and digital back-propagation is also studied. Figure 5 shows the AIR versus transmission distance for different modulation formats in an ideal $C-$band transmission without transceiver noise limitations. Similar to the EDFA-amplified systems, it was found that for DP-QPSK systems with reach up to 10,000 km nonlinear compensation is not

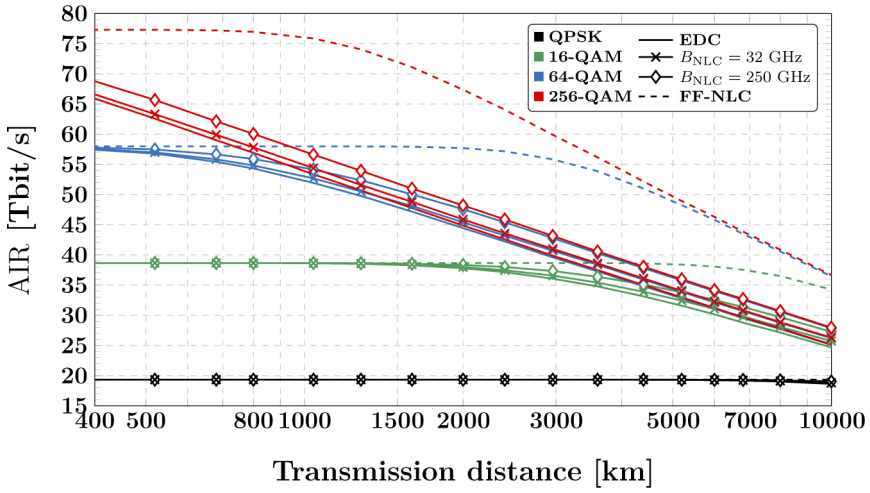

Fig. 3. Achievable information rates (AIRs) versus transmission distances for different modulation formats in EDFA-amplified ideal $C-$band (~4.8 THz) communication systems using multi-channel digital back-propagation (without transceiver noise limitations).

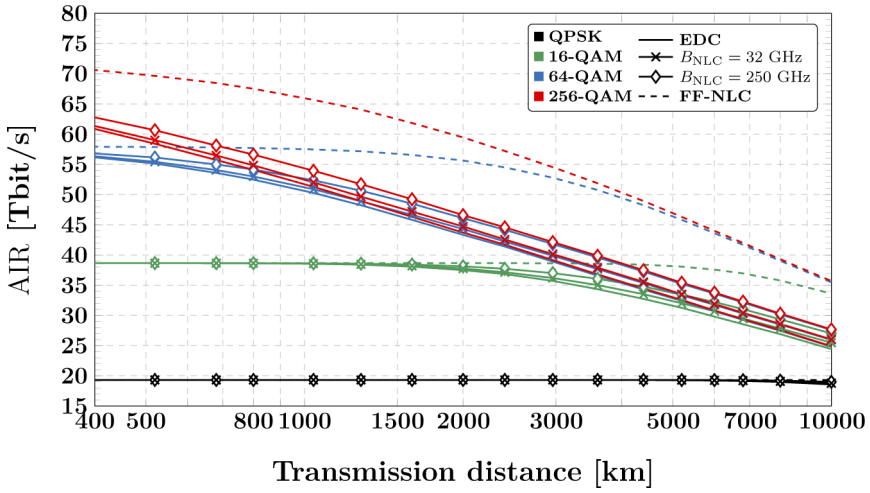

Fig. 4. Achievable information rates (AIRs) versus transmission distances for different modulation formats in EDFA-amplified $C-$band (~4.8-THz) communication systems using multi-channel digital back-propagation (with a transceiver SNR of 25 dB).

Optics EXPRESS

necessary for increasing the AIRs, as the AIRs are always at its saturated maximum value. For DP-16QAM NLC becomes effective in increasing AIR for transmission distances beyond 3000 km. For DP-64QAM nonlinear compensation is essential for distances longer than 1000 km, whereas for DP-256QAM systems NLC would be effective for all considered distances starting from 400 km.

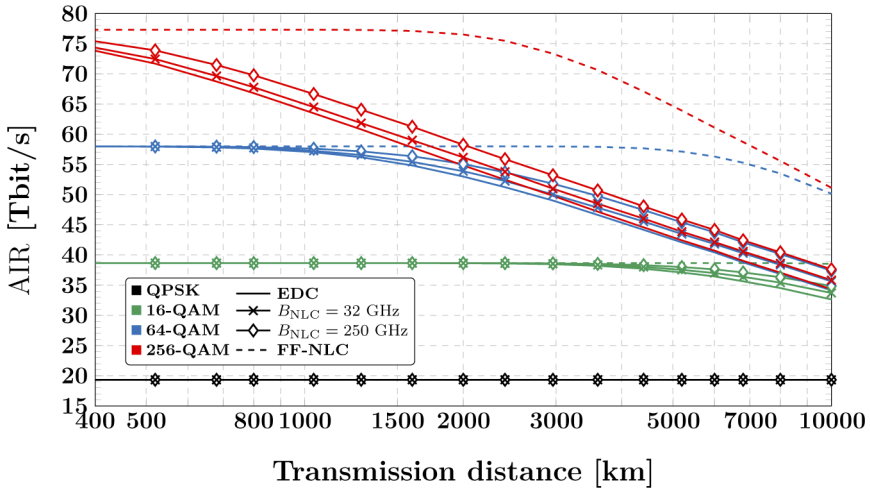

Fig. 5. AIRs in Raman-amplified ideal $C-$band systems using digital back-propagation (without transceiver noise limitations).

We consider the more practical emulation of Raman-amplified $C-$band transmission systems, which accounts for the transceiver SNR limitations, which are again set to 25 dB. Figure 6 shows the AIR versus transmission distance for different modulation formats. Similar to our previous discussions, NLC is not necessary for DP-QPSK transmission for enhancing the AIR when the distances are shorter than 10,000 km. When DP-16QAM modulation is applied, nonlinear compensation effectively increases the AIR at transmission distances exceeding 3000 km. For DP-64QAM the distance at which nonlinear compensation starts being effective is 600 km. For any considered system reach NLC increases the achievable rates when DP-256QAM is applied.

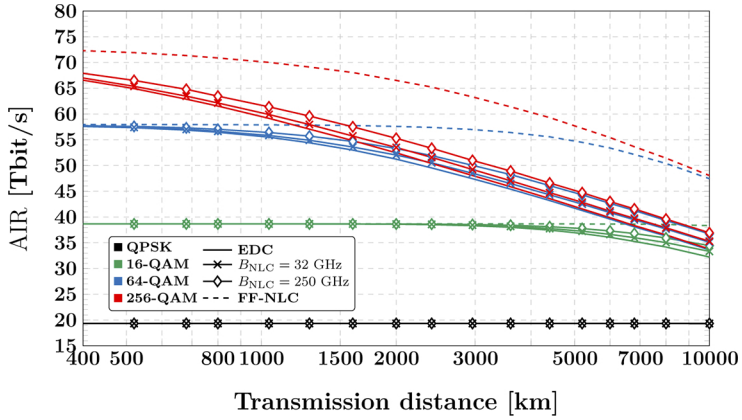

Fig. 6. AIRs in Raman-amplified ideal $C-$band systems using digital back-propagation (with a transceiver SNR of 25 dB).

Optics EXPRESS

3.2. Optical nonlinearity compensation (optical phase conjugation)

As already discussed, applying optical phase conjugation is another promising approach to mitigate nonlinear distortions. In general, the technique facilitates from distributed signal amplification and thus we explore the 1st−order Raman-amplification, which provides a more realistic modelling of fully-loaded C−band transmission systems for both with and without transceivers limited in SNR performance. A mid-link optical phase conjugation is applied.

Figure 7 shows the AIRs as a function of system reach for different modulation formats in the ideal C−band transmission case, where an ideal operation OPC is also applied. After the compensation of the signal-signal nonlinearity, the signal-noise nonlinearity in the ideal OPC scheme arises from the interaction between the signal and the ASE noise in both the first half fibre link and the second half fibre link (after the signal phase conjugation). The second-order signal-noise interaction is also taken into consideration [16,43]. We observe that nonlinear compensation is not required for DP-QPSK systems at the distance up to of 10,000 km since the achievable rates are at their saturated maximum. For DP-16QAM applying OPC is effective in increasing the AIRs when the system reach is beyond 3000 km. For DP-64QAM this distance reduces to 800 km, while for DP-256QAM for any examined distance in the range between 400 and 10,000 km OPC significantly increases the achievable information rates.

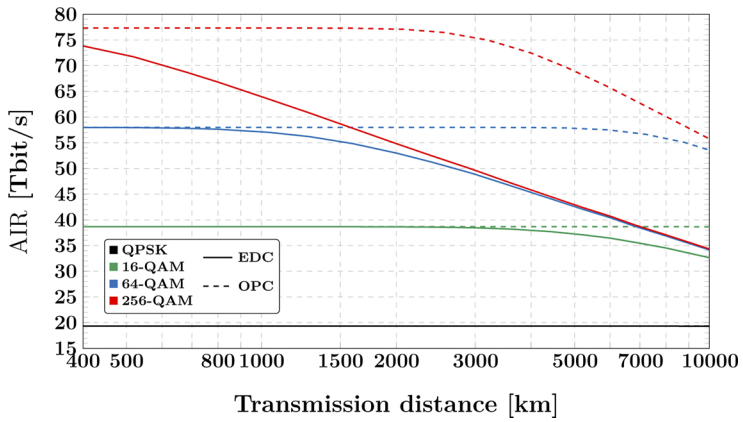

Fig. 7. AIRs in Raman-amplified ideal C−band systems using optical phase conjugation (without transceiver noise limitations and OPC loss).

We further investigate the impact of transceiver noise on the AIR performance in the OPC compensated system. The transceiver SNR is set to 25 dB again with a fully-loaded C−band transmission, and the loss in the OPC device is set to 10 dB which can be compensated using an EDFA. In addition to the signal-noise nonlinearity in the ideal OPC case, here the interaction between the signal and the transceiver noise as well as the additional amplifier noise to compensate for the loss from the non-ideal OPC device is also taken into account. Figure 8 shows the AIR as a function of transmission distance for different modulation formats. The results suggest that for DP-QPSK the degradation of AIR due to transceiver noise is negligible and there is no benefit from nonlinearity compensation at all examined distances up to 10,000 km since the rates are maximal. The transceiver noise effect is also marginal for DP-16QAM systems where OPC becomes beneficial at distances longer than 3000 km, similar to the case of the ideal C−band transmission. The degradation due to the transceiver noise is more substantial for higher-order modulation formats. The distance at which AIR gains are observed for DP-64QAM is around 500 km and for DP-256QAM OPC is effective at all examined distances from 400 to 10,000 km.

It is noted that in this work we have considered a fixed span length of 80 km in both EDFA and Raman amplified optical fibre communication systems, where the performance of DBP

Optics EXPRESS

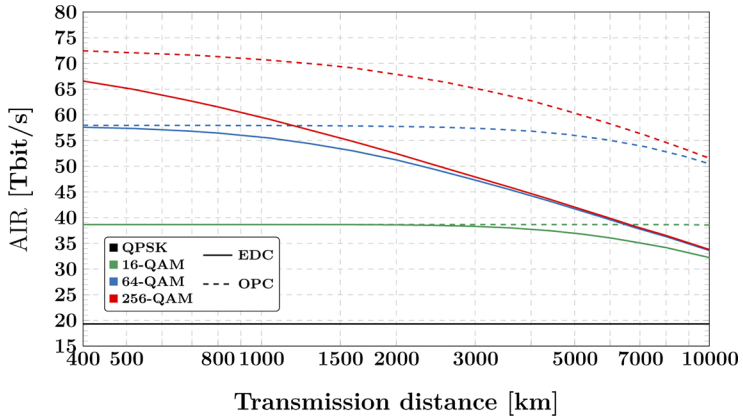

Fig. 8. AIRs in Raman-amplified practical $C-$band systems using optical phase conjugation (with a transceiver SNR of 25 dB and an OPC loss of 10 dB).

and OPC have been analysed. Some reported works have demonstrated that the performance of DBP and OPC can be further improved when the fibre span lengths are optimised [51–54]. In this case, the performance of AIRs versus transmission distances in such optimised systems can also be enhanced correspondingly. It is also worth noting that in practical transmission systems optical phase conjugation cannot realise a full compensation of fibre nonlinearities due to the non-perfectly symmetric power profile and the dispersion slope, since the power and the dispersion profiles are not completely symmetric between the original and conjugated signals. Also, in the EDFA amplified transmission systems, which are the most commonly deployed in current optical network infrastructure, mid-link OPC cannot realise a full compensation of the nonlinear distortions in principle either, since the power profiles in the fibre links before and after OPC are asymmetric. In such systems, the joint application of OPC and DBP would be necessary to optimise the performance of nonlinearity compensation.

4. Conclusions

The gains in AIRs, that can be attained from the use of digital and optical nonlinearity compensation, have been thoroughly investigated in fully-loaded $C-$band ($\sim$ 4.8 THz) Nyquist-spaced WDM optical fibre communication systems, considering different signal modulation formats. Both EDFA and Raman amplification schemes have been applied, and transceiver limitations were included to model a practically-relevant $C-$band transmission system. It was found that, in such wideband transmission schemes, the efficacy of both DBP and OPC in enhancing the AIRs depends on the particular modulation format and transmission distance. The system reach, at which NLC becomes effective, is shorter for higher-order modulation formats. Specifically, for DP-QPSK systems, NLC is not necessary for all investigated transmission distances up to 10,000 km. In addition, transceiver noise arising in practical systems have a marginal impact on the AIRs of DP-QPSK and DP-16QAM systems, while it is always limiting the AIRs more substantially in the case of DP-64QAM and DP-256QAM systems.

Our work provides an insight into the enhancement and application of both digital and optical NLC techniques in fully-loaded $C-$band communication systems with EDFA and Raman amplifications applied, considering practical transceiver limitations.

Funding. Horizon 2020 Framework Programme (101008280); Engineering and Physical Sciences Research Council (EP/J017582/1); British Telecommunications.

Acknowledgments. The authors would like to thank Dr. L. Galdino, Prof. P. Bayvel from University College London (UCL), Dr. G. Saavedra from University of Concepción, Dr. D. Semrau and Dr. D. Lavery from Infinera, Dr. B.

Optics EXPRESS

Karanov, Dr. G. Liga and Dr. A. Alvarado from Eindhoven University of Technology (TU/e), and Dr. M. Tan from Aston University for helpful discussions.

Disclosures. The authors declare that there are no conflicts of interest related to this article.

References

1. "Cisco. Cisco Visual Networking Index: Forecast and Methodology 2017-2022," https://www.cisco.com/c/dam/m/en_us/network-intelligence/service-provider/digital-transformation/knowledge-network-webinars/pdfs/1213-business-services-ckn.pdf (2018).
2. P. Bayvel, R. Maher, T. Xu, G. Liga, N. A. Shevchenko, D. Lavery, A. Alvarado, and R. I. Killey, "Maximizing the optical network capacity," Philos. Trans. R. Soc., A **374**(2062), 20140440 (2016).
3. L. Szczecinski and A. Alvarado, *Bit-interleaved coded modulation: fundamentals, analysis and design* (John Wiley & Sons, 2015).
4. D. Semrau, T. Xu, N. A. Shevchenko, M. Paskov, A. Alvarado, R. I. Killey, and P. Bayvel, "Achievable information rates estimates in optically amplified transmission systems using nonlinearity compensation and probabilistic shaping," Opt. Lett. **42**(1), 121–124 (2017).
5. M. Secondini, E. Forestieri, and G. Prati, "Achievable information rate in nonlinear WDM fiber-optic systems with arbitrary modulation formats and dispersion maps," J. Lightwave Technol. **31**(23), 3839–3852 (2013).
6. T. Fehenberger, A. Alvarado, P. Bayvel, and N. Hanik, "On achievable rates for long-haul fiber-optic communications," Opt. Express **23**(7), 9183–9191 (2015).
7. S. J. Savory, "Digital filters for coherent optical receivers," Opt. Express **16**(2), 804–817 (2008).
8. E. Ip and J. M. Kahn, "Digital equalization of chromatic dispersion and polarization mode dispersion," J. Lightwave Technol. **25**(8), 2033–2043 (2007).
9. G. Colavolpe, T. Foggi, E. Forestieri, and M. Secondini, "Impact of phase noise and compensation techniques in coherent optical systems," J. Lightwave Technol. **29**(18), 2790–2800 (2011).
10. R.-J. Essiambre and R. W. Tkach, "Capacity trends and limits of optical communication networks," Proc. IEEE **100**(5), 1035–1055 (2012).
11. P. P. Mitra and J. B. Stark, "Nonlinear limits to the information capacity of optical fibre communications," Nature **411**(6841), 1027–1030 (2001).
12. T. Xu, N. A. Shevchenko, D. Lavery, D. Semrau, G. Liga, A. Alvarado, R. I. Killey, and P. Bayvel, "Modulation format dependence of digital nonlinearity compensation performance in optical fibre communication systems," Opt. Express **25**(4), 3311–3326 (2017).
13. R. Dar and P. J. Winzer, "On the limits of digital back-propagation in fully loaded WDM systems," IEEE Photonics Technol. Lett. **28**(11), 1253–1256 (2016).
14. D. Rafique and A. D. Ellis, "Various nonlinearity mitigation techniques employing optical and electronic approaches," IEEE Photonics Technol. Lett. **23**(23), 1838–1840 (2011).
15. A. Ellis, S. Le, M. Al-Khateeb, S. Turitsyn, G. Liga, D. Lavery, T. Xu, and P. Bayvel, "The impact of phase conjugation on the nonlinear-shannon limit: The difference between optical and electrical phase conjugation," in *2015 IEEE Summer Topicals Meeting Series*, (IEEE, 2015), pp. 209–210.
16. M. A. Z. Al-Khateeb, M. McCarthy, C. Sánchez, and A. Ellis, "Effect of second order signal–noise interactions in nonlinearity compensated optical transmission systems," Opt. Lett. **41**(8), 1849–1852 (2016).
17. E. Temprana, E. Myslivets, B.-P. Kuo, L. Liu, V. Ataie, N. Alic, and S. Radic, "Overcoming Kerr-induced capacity limit in optical fiber transmission," Science **348**(6242), 1445–1448 (2015).
18. R. Maher, T. Xu, L. Galdino, M. Sato, A. Alvarado, K. Shi, S. J. Savory, B. C. Thomsen, R. I. Killey, and P. Bayvel, "Spectrally shaped DP-16QAM super-channel transmission with multi-channel digital back-propagation," Sci. Rep. **5**(1), 8214 (2015).
19. M. Stephens, M. Tan, I. Phillips, S. Sygletos, P. Harper, and N. J. Doran, "1 THz-bandwidth polarization-diverse optical phase conjugation of 10×114Gb/s DP-QPSK WDM signals," in *Optical Fiber Communication Conference*, (Optical Society of America, 2014), pp. W3F–6.
20. T. Umeki, T. Kazama, A. Sano, K. Shibahara, K. Suzuki, M. Abe, H. Takenouchi, and Y. Miyamoto, "Simultaneous nonlinearity mitigation in 92×180-Gbit/s PDM-16QAM transmission over 3840 km using PPLN-based guard-band-less optical phase conjugation," Opt. Express **24**(15), 16945–16951 (2016).
21. I. D. Phillips, M. Tan, M. F. C. Stephens, M. E. McCarthy, E. Giacoumidis, S. Sygletos, P. Rosa, S. Fabbri, S. T. Le, T. Kanesan, S. K. Turitsyn, N. J. Doran, P. Harper, and A. D. Ellis, "Exceeding the nonlinear-shannon limit using raman laser based amplification and optical phase conjugation," in *Optical Fiber Communication Conference*, (Optical Society of America, 2014), p. M3C.1.
22. J. C. Cartledge, F. P. Guiomar, F. R. Kschischang, G. Liga, and M. P. Yankov, "Digital signal processing for fiber nonlinearities," Opt. Express **25**(3), 1916–1936 (2017).
23. M. P. Yankov, H. E. Hansen, F. Da Ros, P. M. Kaminski, E. P. da Silva, M. Galili, L. K. Oxenløwe, and S. Forchhammer, "Probabilistic shaping for the optical phase conjugation channel," IEEE J. Sel. Top. Quantum Electron. **27**(2), 1–16 (2021).
24. F. Da Ros, M. Lillieholm, M. P. Yankov, P. Guan, H. Hu, S. Forchhammer, M. Galili, and L. Oxenl, "Impact of signal-conjugate wavelength shift on optical phase conjugation-based transmission of QAM signals," in *European Conference on Optical Communication*, (IEEE, 2017), pp. 1–3.

Optics EXPRESS

25. W. Shieh and X. Chen, "Information spectral efficiency and launch power density limits due to fiber nonlinearity for coherent optical OFDM systems," IEEE Photonics J. **3**(2), 158–173 (2011).
26. T. Xu, N. A. Shevchenko, B. Karanov, D. Lavery, L. Galdino, A. Alvarado, R. I. Killey, and P. Bayvel, "Nonlinearity compensation and information rates in fully-loaded C-band optical fibre transmission systems,"in *Proceedings of IEEE European Conference on Optical Communication*, (IEEE, 2017), pp. 1–3.
27. T. Xu, N. A. Shevchenko, Z. Li, T. Liu, and P. Bayvel, "Limit of achievable information rates in EDFA and raman amplified transmission systems using nonlinearity compensation," in *Proceedings of IEEE International Conference on Transparent Optical Networks*, (IEEE, 2019), p. Fr.D4.3.
28. P. Poggiolini, "The GN model of non-linear propagation in uncompensated coherent optical systems," J. Lightwave Technol. **30**(24), 3857–3879 (2012).
29. P. Johannisson and M. Karlsson, "Perturbation analysis of nonlinear propagation in a strongly dispersive optical communication system," J. Lightwave Technol. **31**(8), 1273–1282 (2013).
30. R. Dar, M. Feder, A. Mecozzi, and M. Shtaif, "Inter-channel nonlinear interference noise in wdm systems: modeling and mitigation," J. Lightwave Technol. **33**(5), 1044–1053 (2015).
31. L. Galdino, D. Semrau, D. Lavery, G. Saavedra, C. B. Czegledi, E. Agrell, R. I. Killey, and P. Bayvel, "On the limits of digital back-propagation in the presence of transceiver noise," Opt. Express **25**(4), 4564–4578 (2017).
32. S. R. Chinn, "Analysis of counter-pumped small-signal fibre Raman amplifiers," Electron. Lett. **33**(7), 607–608 (1997).
33. C. R. Giles and E. Desurvire, "Modeling erbium-doped fiber amplifiers," J. Lightwave Technol. **9**(2), 271–283 (1991).
34. G. P. Agrawal, *Fiber-optic communication systems* (John Wiley & Sons, 2010).
35. J. Bromage, "Raman amplification for fiber communications systems," J. Lightwave Technol. **22**(1), 79–93 (2004).
36. I. S. Gradshteyn and I. M. Ryzhik, *Table of integrals, series, and products* (Academic, 2014).
37. N. A. Shevchenko, T. Xu, C. Jin, D. Lavery, R. I. Killey, and P. Bayvel, "Information rate in ultra-wideband optical fiber communication systems accounting for high-order dispersion," arXiv preprint arXiv:1905.10246 (2019).
38. A. Carena, V. Curri, G. Bosco, P. Poggiolini, and F. Forghieri, "Modeling of the impact of nonlinear propagation effects in uncompensated optical coherent transmission links," J. Lightwave Technol. **30**(10), 1524–1539 (2012).
39. R. Dar, M. Feder, A. Mecozzi, and M. Shtaif, "Properties of nonlinear noise in long, dispersion-uncompensated fiber links," Opt. Express **21**(22), 25685–25699 (2013).
40. R. Dar, M. Feder, A. Mecozzi, and M. Shtaif, "Accumulation of nonlinear interference noise in fiber-optic systems," Opt. Express **22**(12), 14199–14211 (2014).
41. D. Rafique and A. D. Ellis, "Impact of signal-ASE four-wave mixing on the effectiveness of digital back-propagation in 112 Gb/s PM-QPSK systems," Opt. Express **19**(4), 3449–3454 (2011).
42. L. Beygi, N. V. Irukulapati, E. Agrell, P. Johannisson, M. Karlsson, H. Wymeersch, P. Serena, and A. Bononi, "On nonlinearly-induced noise in single-channel optical links with digital backpropagation," Opt. Express **21**(22), 26376–26386 (2013).
43. N. A. Shevchenko, T. Xu, D. Lavery, G. Liga, D. J. Ives, R. I. Killey, and P. Bayvel, "Modeling of nonlinearity-compensated optical communication systems considering second-order signal-noise interactions," Opt. Lett. **42**(17), 3351–3354 (2017).
44. N. A. Shevchenko, T. Xu, D. Semrau, G. Saavedra, G. Liga, M. Paskov, L. Galdino, A. Alvarado, R. I. Killey, and P. Bayvel, "Achievable information rates estimation for 100-nm Raman-amplified optical transmission system," in *Proceedings of IEEE European Conference on Optical Communication*, (VDE, 2016), pp. 1–3.
45. H. Hu, R. M. Jopson, A. H. Gnauck, S. Randel, and S. Chandrasekhar, "Fiber nonlinearity mitigation of WDM-PDM QPSK/16-QAM signals using fiber-optic parametric amplifiers based multiple optical phase conjugations," Opt. Express **25**(3), 1618–1628 (2017).
46. M. A. Z. Al-Khateeb, M. Tan, M. A. Iqbal, A. Ali, M. E. McCarthy, P. Harper, and A. D. Ellis, "Experimental demonstration of 72% reach enhancement of 3.6Tbps optical transmission system using mid-link optical phase conjugation," Opt. Express **26**(18), 23960–23968 (2018).
47. P. Poggiolini, G. Bosco, A. Carena, V. Curri, Y. Jiang, and F. Forghieri, "The GN-model of fiber non-linear propagation and its applications," J. Lightwave Technol. **32**(4), 694–721 (2014).
48. W. Zeiler, F. Di Pasquale, P. Bayvel, and J. E. Midwinter, "Modeling of four-wave mixing and gain peaking in amplified WDM optical communication systems and networks," J. Lightwave Technol. **14**(9), 1933–1942 (1996).
49. R. E. Caflisch, "Monte Carlo and quasi-Monte Carlo methods," Acta Numerica **7**, 1–49 (1998).
50. K. Shi, E. Sillekens, and B. C. Thomsen, "246 GHz digitally stitched coherent receiver," in *Optical Fiber Communication Conference*, (Optical Society of America, 2017), pp. M3D–3.
51. B. Karanov, T. Xu, N. A. Shevchenko, D. Lavery, R. I. Killey, and P. Bayvel, "Span length and information rate optimisation in optical transmission systems using single-channel digital backpropagation," Opt. Express **25**(21), 25353–25362 (2017).
52. P. Rosa, S. T. Le, G. Rizzelli, M. Tan, and J. D. Ania-Castañón, "Signal power asymmetry optimisation for optical phase conjugation using raman amplification," Opt. Express **23**(25), 31772–31778 (2015).
53. P. Rosa, G. Rizzelli, and J. D. Ania-Castañón, "Link optimization for dwdm transmission with an optical phase conjugation," Opt. Express **24**(15), 16450–16455 (2016).
54. G. Rizzelli, P. Rosa, P. Corredera, and J. D. Ania-Castañón, "Transmission span optimization in fiber systems with cavity and random distributed feedback ultralong raman laser amplification," J. Lightwave Technol. **35**(22), 4967–4972 (2017).